Research Article

Journal of RAMAN SPECTROSCOPY

Received: 26 June 2008 Accepted: 14 August 2008 Published online in Wiley Interscience:

(www.interscience.com) DOI 10.1002/jrs.2124

Experimental study of the vibrational spectra of $(CH_3)_3GeBr$ supported by DFT calculations

M. L. Roldán, S. A. Brandán and A. Ben Altabef*,†

The infrared and Raman spectra of bromotrimethylgermane (BTMG) were recorded afresh to complete the assignment of its vibrational spectra. The vibrational spectrum of BTMG has been predicted from hybrid density functional theory calculations (B3LYP) with several basis sets. The resulting harmonic wavenumbers were scaled by Pulay's scaled quantum mechanical (SQM) and the wavenumber-linear scaling (WLS) methods to obtain accurate force fields which could aid in the vibrational assignment. Low-temperature infrared techniques together with Fourier self-deconvolution (FSD) on the Raman spectrum were used to improve the resolution of the spectra for the modes that could not be observed before. An SQM analysis was carried out to obtain the valence force constants and a set of scale factors that best reproduced the experimental data.

Supporting information may be found in the online version of this article.

Keywords: bromotrimethylgermane; vibrational spectra; force field; Fourier-self deconvolution

Introduction

Bromotrimethylgermane (Me_3GeBr, BTMG) can be prepared by the bromination of Me_4Ge with HBr under pressure[1] or by boiling it with bromine for a few hours.[2] Jointly with the chloro compound, BTMG is widely used in organic synthetic applications. It is routinely used as trimethylgermyl-reagent in reactions such as the formation of dienolates of α, β-unsaturated esters which react with electrophiles at the γ-position,[3] synthesis of (germyl)-allyl phosphines, where the trimethylgermyl group can act as a protecting group of the phosphorous center after selective reactions involving the allyl groups[4] and as reagent for cyclopentannulation reactions.[5] In addition, it is used to produce $(CH_3)_3Ge^+$ cations in gas-phase reactions for differentiation of *cis*- and *trans*-1,2- cyclopentadienol isomers in triple-quadrupole mass spectroscopy,[6] with the advantage of being more sensitive and selective than the C, Si or Sn analogs. The molecular structure of BTMG was initially determined using microwave spectroscopy by Li and Durig.[7] Recently, the full geometry of this compound, as well as of the chloro compound, was resolved by Aarset and Page[8] through gas-phase electron diffraction supported by theoretical calculations. The Raman spectrum of BTMG was first measured by Batuev *et al*.[9] and Mironov *et al*.[10] but without any assignment of the observed bands. Later, Van de Vondel *et al*.[11] recorded the infrared and Raman spectra, assigning some of the fundamental bands but making no distinction between the CH modes of closer wavenumbers, which were assigned to a single band. Durig *et al*.[12] recorded the far-infrared and the Raman spectrum of the solid in order to find the torsional modes which were not observed earlier. Unfortunately, all the bands found in these measurements belong to the librational modes. Imai *et al*.[13] recorded the infrared and Raman spectra of the $(CH_3)_3MX$ (M = Ge, Sn; X = Cl, Br) series and their deuterated species. Through a normal coordinate analysis of both isotopic species of each compound carried out by these authors, the force constants of the molecules were calculated. However, a large number of fundamental bands remained unassigned.

The goal of this work is to identify the unresolved bands and achieve a complete assignment by combining the experimental information obtained from low-temperature infrared (LTIR) techniques and the application of Fourier self-deconvolution (FSD) on the Raman spectra, with that obtained from the theoretical calculations. The force field of BTMG calculated with the B3LYP/6-31G* was scaled to obtain the corresponding wavenumbers, and then to simulate the vibrational spectra using two different methodologies in the scaling procedure: (1) the scaled quantum mechanical (SQM) method of Pulay[14–16] and (2) the Yoshida's wavenumber linear-scaling method[17] which was defined for compounds containing heavy atoms including germanium. Additionally, the internal force constants were calculated by using the Kalincsák and Pongor[18] scale factors and the B3LYP/6-31G* force field.

Experimental

A commercial sample of BTMG was purchased from ABCR (98% purity). The liquid was used without additional purification and handled avoiding atmospheric humidity. The infrared spectra were recorded on a Fourier transform infrared (FTIR) spectrophotometer, Perkin Elmer Model GX1, in the range 4000–400 cm^{-1}, with a resolution of 2 cm^{-1} and 64 scans. The FTIR spectra of the gas, liquid and solid phases were registered. The LTIR measurements were recorded by cooling the sample from room temperature to

* *Correspondence to: A. Ben Altabef, Instituto de Química Física, Facultad de Bioquímica, Química y Farmacia, Universidad Nacional de Tucumán, San Lorenzo 456, T4000CAN Tucumán, R. Argentina.*
E-mail: altabef@fbqf.unt.edu.ar

† *Member of the Carrera del Investigador Científico, CONICET (R. Argentina).*

Instituto de Química Física, Facultad de Bioquímica, Química y Farmacia, Universidad Nacional de Tucumán, San Lorenzo 456, T4000CAN Tucumán, R. Argentina

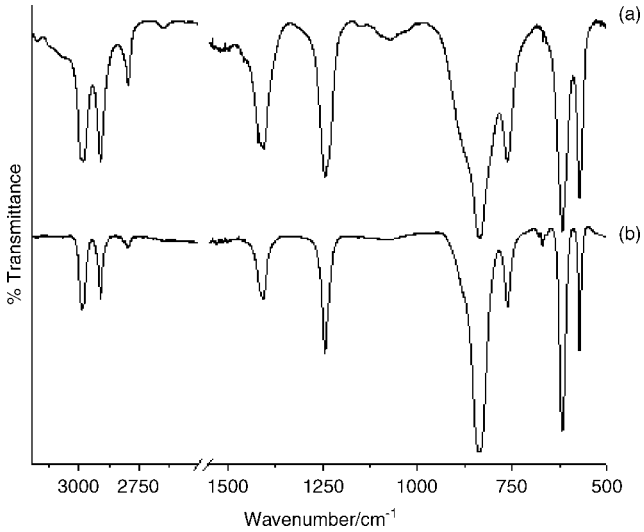

Figure 1. (a) Gas and (b) liquid phase infrared spectra at room temperature.

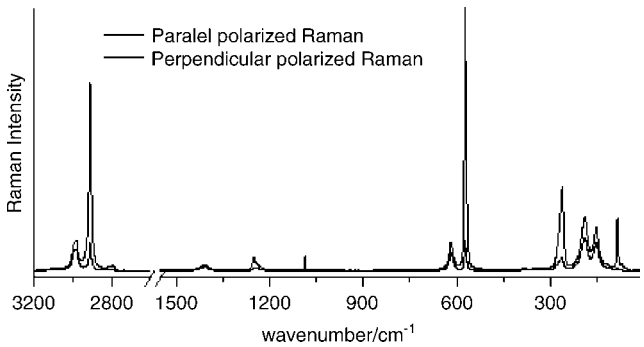

Figure 2. Overlaid parallel and perpendicular polarized Raman spectra.

liquid nitrogen temperature by using a variable-temperature RIIC (VLT-2) cell equipped with AgCl windows. The room-temperature infrared (RTIR) spectrum was recorded as a film between KBr windows. The parallel and perpendicular polarized Raman spectra of the sample were recorded with an FT-Raman Bruker RFS 100 spectrophotometer, equipped with an Nd : YAG laser (excitation line1064 nm) and a liquid-N_2-cooled Ge detector, with a resolution of 1 cm^{-1} and 200 scans. The depolarization ratios were calculated from those of the fundamental band intensities in both spectra. The infrared spectra of gaseous and liquid BTMG are displayed in Fig. 1, and the overlaid parallel and perpendicular polarized Raman spectra are shown in Fig. 2. The measured vibrational wavenumbers in the infrared and Raman spectra and their assignment to the vibrational normal modes of the molecule are summarized in Table 1.

Spectral analysis

FSD is based on the method described by Kauppinen *et al.*[19–21] where by defining only two enhancement factors *W* (bandwidth at half-height) and *K* (ratio of bandwidth of the enhanced and original bands) better-resolved bands were obtained. This procedure was applied to the analysis of the Raman spectra by using Gaussian peak shapes and was performed using the standard software of the infrared spectrophotometer.[22]

Computational Details

The Gaussian03 program[23] was used to carry out all the density function theory (DFT) calculations. The C_{3V} molecular symmetry and the experimental geometrical parameters determined by gas-phase electron diffraction (GED) experiments[8] for BTMG were used as initial geometry for the vibrational frequency calculations. For this task, the Becke's three-parameter hybrid functional B3LYP and the 6-31G, 6-31G*, 6-31+G, 6-31+G*, 6-311G, 6-311G*, 6-311+G, 6-311+G*, 6-311+G** and 6-311++G** split valence basis sets were selected. The performance in the prediction of the vibrational wavenumbers of cc-pVDZ and cc-pVTZ basis sets of Dunning and coworkers[24–27] as well as the Lanl2dz and Lanl2dzdp effective core potential (ECP) on Ge and Br atom basis sets were also tested. The theoretical wavenumbers obtained from the above-mentioned calculations for the fundamental modes are shown in Table S1 (Supporting Information). The departures from these values to the experimental wavenumbers were measured by the root-mean square deviation (RMSD). The quantum mechanical force field was calculated with the B3LYP/6-31G* combination. A standard program was used to convert the resulting force field from Cartesian to symmetry coordinates by using the coordinates proposed by Pulay *et al.*[28] which are defined in Table S2 (Supporting Information). Then, the scaling force field was made using the SQM methodology proposed by Pulay *et al.*[14–16] which is based on the following equation:

$$F'_{ij} = (\lambda_i.\lambda_j)^{1/2} F_{ij} \quad (1)$$

The scaling procedure was made by multiplying the diagonal force constants (F_{ij}) corresponding to a particular symmetry coordinate by the scale factors (λ_i, λ_j) determined by a least-squares fit of the experimental wavenumbers. Thus, the off-diagonal force constants result automatically scaled by the geometric mean of these factors. F'_{ij} is the resulting scaled force constant. The scale factor adjustments (refinement procedure) were performed by an iterative method to obtain the calculated wavenumbers as close as possible to the experimental ones. In this procedure, the weight for vibrational modes of the A_1 and *E* symmetry was taken as unity, and that for the inactive A_2 modes as zero. The scaled force constant matrix in terms of symmetry coordinates is presented in Table S3 (Supporting Information). The SQM force field was also used to obtain the potential energy distribution (PED) and to calculate the valence force constants expressed in internal coordinates. The force constant conversion, fitting of the scale factors and PED calculation were carried out with the program FCARTP.[29]

Vibrational Results

The C_{3v} symmetry predicted for the BTMG by quantum mechanical calculations (Fig. 3) is consistent with the structure determined by Aarset *et al.*[8] using the GED technique. The 36 vibrational normal modes are classified according to $8A_1$ (IR, R) + $4A_2$ + $12E$ (IR, R). The Raman inactive modes (A_2) are forbidden by selection rules. Table S1 lists the harmonic wavenumbers resulting from the calculations along with the measured wavenumbers taken from the LTIR spectrum and from the Raman spectrum below 400 cm^{-1}.

Theoretical prediction of the vibrational spectra

The vibrational wavenumbers predicted for BTMG by the DFT calculations and different basis sets are listed in Table S1. From a

Table 1. Observed bands (in cm^{-1}) in the infrared and Raman spectra of BTMG

Infrared[a]			Raman				
	Liquid						
Gas	Room temperature	Low temperature[b]	Observed[c]	Depolarization ratio[d]		Assignment[e]	
		2993w	2992sh		ν_{13}	ν_a CH_3	E
2988	2988m	2988w	2988sh		ν_1	ν_a CH_3	A_1
2983m	2984sh	2983m	2984(11)	0.74Dp	ν_{14}	ν_a CH_3	E
2911m	2911m	2911w	2911(70)	0.15P	ν_2	ν_s CH_3	A_1
		2908			ν_{15}	ν_s CH_3	E
1420m		1420	1422[f] sh		ν_3	δ_a CH_3	A_1
	1407m	1412m	1412[f] (2)	0.75Dp	ν_{16}	δ_a CH_3	E
1405m		1402	1405[f] sh		ν_{17}	δ_a CH_3	E
1244m	1244s	1246	1252[f] (5)	0.22P	ν_4	δ_s CH_3	A_1
1234sh	1237sh	1235	1242[f] sh		ν_{18}	δ_s CH_3	E
		844vs			ν_{19}	ρ CH_3	E
835s	838vs	830sh	828(0.6)	0.25P	ν_5	ρ CH_3	A_1
761m	762m	767s	761(0.6)	0.45Dp	ν_{20}	ρ CH_3	E
618f	618vs	620vs	618(11)	0.63Dp	ν_{21}	ν_a GeC_3	E
572m	572m	573s	573(100)	0.12P	ν_6	ν_s GeC_3	A_1
–	–	–	262(31)	0.17P	ν_7	ν GeBr	A_1
–	–	–	192(20)	0.65Dp	ν_{22}	δ_a GeC_3	E
–	–	–	153(16)	0.64Dp	ν_{23}	ρ GeC_3	E
	–	–	122(3)	0.45Dp	ν_{24}	τ CH_3	E

[a] w, weak; m, medium; s, strong; vs, very strong; sh, shoulder.
[b] From the Infrared spectra cooled to the nitrogen liquid temperature.
[c] Relative intensity in parentheses.
[d] p, polarized; dp, depolarized.
[e] ν, stretching; δ, angular deformation; ρ, rocking; τ, torsion; s, symmetric; a, antisymmetric.
[f] From Fourier self-deconvolution (Fig. S4).

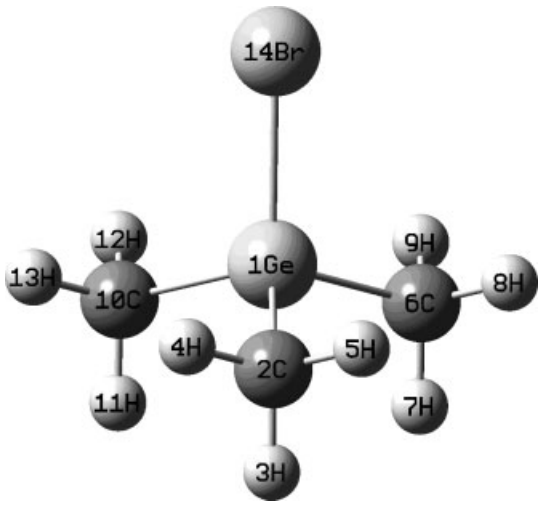

Figure 3. Molecular geometry of BTMG showing the labeling of the atoms.

comparison of all the basis sets used, it can be seen that an increase of the basis set size results in a significant improvement in the quality of the calculated wavenumbers. As a result, the split valence basis sets 6-311+G** (RMSD = 71.9 cm^{-1}) and 6-311++G** (RMSD = 72.0 cm^{-1}) deviate less from the experimental data than the other basis sets tested. The Dunning basis sets[24–27] (cc-pVDZ, cc-pVTZ) give wavenumbers with the same quality (RMSD = 72.5 cm^{-1} and RMSD = 72.7 cm^{-1}, respectively) of the split valence basis sets, and the use of the effective core potential (ECP) basis sets (lanl2dz, lanl2dzdp) does not result in any improvement in the wavenumber calculation. These deviations from the experimental data could be further reduced by scaling the force field with factors to achieve an even closer description of the observed vibrational spectra.

The development of different scaling methods in the last decades[14,17,18,30] has increased the accuracy in the prediction of the vibrational spectra, thereby helping their interpretation. These methodologies are based on fitting the theoretical wavenumbers to the experimental ones to reproduce the molecular spectral profile as well as possible. Hence, the vibrational spectrum was predicted mainly using two methodologies, the SQM proposed by Pulay *et al.*[14] and Rauhut and Pulay[15,16] for B3LYP/6-31G* force field (described in the Calculations Section) and the WLS proposed by Yoshida *et al.*[17] for the B3LYP/6-311+G** force field. The WLS method is based on the linear equation

$$\nu_{obs}/\nu_{calc} = 1.0087(9) - 0.0000163(6)\nu_{calc} \quad (2)$$

where ν_{obs} and ν_{calc} are given in wavenumbers (cm^{-1}). Each scale factor, defined as ν_{obs}/ν_{calc}, is applied to the corresponding calculated wavenumber (ν_{calc}). In the SQM scaling, two sets of scale factors were used to predict the experimental data: those proposed by Rauhut and Pulay[15] for molecules containing elements of the first period of the periodic table, and those proposed by Kalincsák and Pongor[18] extended for elements of

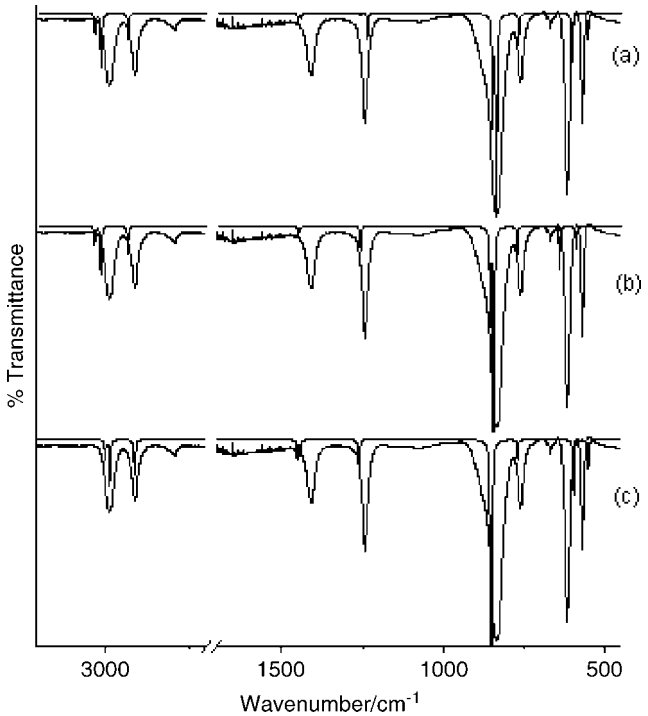

Figure 4. Experimental (continuous line) and predicted (dotted line) IR spectra for BTMG by the SQM method from B3LYP/6-31G* force field using (a) Rauhut and Pulay's scale factors and (b) Kalincsák and Pongor's scale factors, and by (c) the wavenumber-linear scaling of Yoshida from B3LYP/6-311+G**.

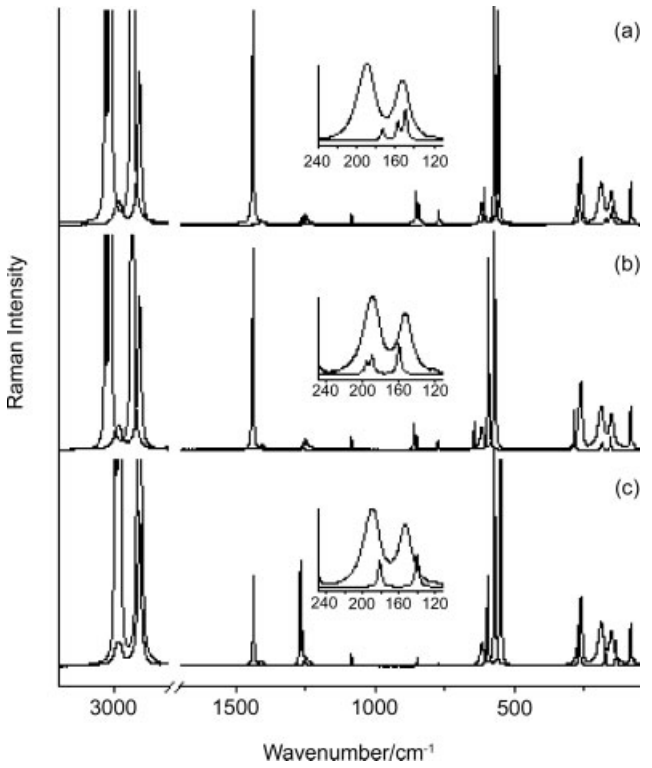

Figure 5. Experimental (continuous line) and predicted (dotted line) Raman spectra for BTMG by the SQM method from B3LYP/6-31G* force field using (a) Rauhut and Pulay's scale factors and (b) Kalincsák and Pongor's scale factors, and by (c) the wavenumber-linear scaling of Yoshida from B3LYP/6-311+G**.

the second row. The vibrational wavenumbers estimated from the SQM procedure with both Rauhut and Pulay's[15] and Kalincsák and Pongor's[18] scale factors using the B3LYP/6-31G* method are given in Table S4 (Supporting Information), where they are compared to the unscaled wavenumbers and the experimental ones. This table also presents the wavenumbers obtained after the scaling with the method of Yoshida *et al*.[17] applied to the B3LYP/6-311+G** force field. The resulting scaled wavenumbers were used to simulate the infrared and Raman spectra for the BTMG molecule for each methodology using the relative intensities predicted for the corresponding theoretical calculation. Thus Figs 4 and 5 show IR and Raman experimental spectra of the liquid compared to the corresponding predicted scaled spectra using the SQM methodology with (1) the Rauhut and Pulay[15] scale factors and (2) the Kalincsák and Pongor[18] scale factors, with the calculated B3LYP/6-31G* intensities. Also (3) the Yoshida equation and the intensities from B3LYP/6-311+G** method are displayed. Clearly, the larger deviations of the C–H vibrational modes are significantly reduced after the scaling procedure. Better results were obtained with the WLS method for the C–H stretching modes, as can also be observed from Table S4. The prediction of the C–H deformation and rocking vibrations is nearly the same for all the scaling methods, as can be seen in Figs 4 and 5. The relative intensities estimated from the calculation are somewhat different from the experimental data. For the infrared spectra, both 6-31G* and 6-311+G** calculations estimate the C–H deformation modes of lower intensity, whereas the C–H rocking modes of higher intensity, compared to the observed spectra. In the Raman spectra, the intensity predicted for the C–H modes was too high in all the cases. For the spectral region that involves GeC_3 motions, the prediction became somewhat better for the SQM scaling using the Rauhut and Pulay[15] scale factors. The wavenumbers predicted using the Kalincsák and Pongor[18] transferred scale factors are about 20 cm^{-1} higher than the observed wavenumbers even for the ν(GeBr) stretching, and those predicted by the Yoshida scaling are underestimated, especially for the GeC_3 rocking mode (Table S4). The calculations predict lower intensities for these modes in the infrared spectra as well as in the Raman spectra.

The WLS-scaled IR spectrum using the intensities predicted by B3LYP/6-311+G** calculation together with the gas, liquid and solid spectra for the regions 3050 to 2850 cm^{-1}, 1500 to 1150 cm^{-1} and 1000 to 500 cm^{-1} are shown for comparison in Figs. S1, S2 and S3 (Supporting Information), respectively. The resulting spectral profiles will be discussed in the following section.

Band Assignments

The assignment proposed by previous authors[11,13] for the observed bands in the vibrational spectra is shown in Table S5 (Supporting Information) and is compared with the bands measured by us. Previous assignments, wavenumbers and intensities predicted by the calculations and simulated vibrational spectra obtained using the different sets of scale factors were taken into account to assign the experimental wavenumbers to the fundamental modes of the molecule. The observed bands in the infrared and Raman spectra, as well as their relative intensities, polarization ratios and the proposed assignments are given in Table 1.

Journal of RAMAN SPECTROSCOPY

Methyl Group Modes

Stretching modes

In previous reports, the symmetric and antisymmetric stretching modes were assigned to two bands in the 3000–2900 cm^{-1} region (Table S5); however, as a result of the vibrational analysis, five infrared active bands belonging to the C–H antisymmetric (ν_{13}, ν_1 and ν_{14}) and symmetric (ν_2 and ν_{15}) modes should be observed. In the RTIR spectra of the liquid, the C–H antisymmetric modes produce a medium intensity band with two peaks at 2988 and 2984 cm^{-1}. In the gas-phase spectra, these bands appear as broad and more intense features at nearly equal frequency. Their counterpart in the Raman spectrum appears as a depolarized band at 2984 cm^{-1} with two shoulders at higher wavenumbers (2988 and 2992 cm^{-1}). In addition, three well-defined bands can be observed in the LTIR as shown in Fig. S1. For the assignment of these bands, the wavenumber values predicted for the WSL scaling given in Table S4 were examined. In Fig. S1 the bands predicted by Yoshida's equation for this region can be seen. The calculation predicts two bands, one belonging to the ν_{13} antisymmetric mode and the other to the pair of ν_1 and ν_{14} antisymmetric modes, which appear overlapped because of the small splitting (2 cm^{-1}) predicted by the calculation. Therefore, the bands in the LTIR that appear at 2993, 2988 and 2983 cm^{-1} can be assigned to ν_{13}, ν_1 and ν_{14} antisymmetric modes, respectively. On the other hand, the two C–H symmetric modes originate a band at 2911 cm^{-1} in the RTIR spectra of both the liquid and the gas phase, which correspond with a strongly polarized band at the same wavenumber in the Raman spectrum. As shown in Fig. S1, this band is resolved into two bands located at 2911 and 2908 cm^{-1} in the LTIR, which, according to the predicted wavenumbers by using the WLS scaling, can be assigned to the ν_2 and ν_{15} symmetric modes, respectively.

The relative intensities predicted by the B3LYP/6-31G* calculation are similar to those of the solid spectrum; however, these are only comparable with those of the gas-phase spectrum.

Deformation modes

The number of bands expected for the C–H deformation modes is five, as well as for the C–H stretching modes. Three of them are antisymmetric and two symmetric. The antisymmetric modes were observed in the infrared spectra by Van de Vondel *et al.*[11] at 1405 cm^{-1} (Imai *et al.*[13]: 1413 cm^{-1}) and the symmetric ones at 1243 cm^{-1} (Imai *et al.*[13]: 1248 cm^{-1}). In the infrared spectra of the liquid sample of BTMG, these bands with medium intensities were located at 1407 and 1244 cm^{-1} with a shoulder at 1237 cm^{-1}. The bands observed in the gas-phase spectrum are rather more intense and broader than those for the liquid spectrum. The appearance of a shoulder at 1405 cm^{-1} was detected in addition to the bands located at 1420 and 1244 cm^{-1} with a shoulder at 1234 cm^{-1}. From an inspection of the wavenumbers estimated by the WLS scaling (Table S4), it can be observed that these bands were calculated to be shifted by about 30 cm^{-1} from the experimental values and this tendency is already shown for the SQM scaling method with both sets of scale factors. Taking into consideration the relative position and the splitting predicted by Yoshida's scaling for the asymmetric modes (Fig. S2), the band located at 1420 cm^{-1} in the gas spectrum was assigned to the ν_3 deformation mode and the shoulder at 1405 cm^{-1} was assigned to the ν_{16} and ν_{17} modes. The bands due to the symmetric deformation are predicted by the calculations to be split by only 1 cm^{-1}; therefore a single band appears in this region in Fig. S2. The band observed at 1244 cm^{-1} with a shoulder at 1234 cm^{-1} can be assigned to the ν_4 and ν_{18} symmetric deformation modes.

On the other hand, the Raman spectra show two broad bands with several shoulders in this region. In order to find the component bands, FSD was applied to this spectral region, and the resulting wavenumbers are listed in Table 1. The resulting deconvoluted spectra show the appearance of three bands at 1422, 1412 and 1405 cm^{-1}, which would correspond to ν_3, ν_{16} and ν_{17} antisymmetric deformation modes, and two bands at 1252 and 1242 cm^{-1} which would assigned to ν_4 and ν_{18} symmetric deformation, respectively (as can be seen in Fig. S4). In addition, the spectrum of the solid (Fig. S2) displays three well-defined bands at 1420, 1412 and 1402 cm^{-1}. According to Yoshida's scaling, these bands can be assigned to the ν_3, ν_{16} and ν_{17} modes, respectively, in excellent agreement with those found in the Raman spectra. Also, the symmetric modes were resolved into two bands at 1246 and 1235 cm^{-1} because of the ν_4 and the ν_{18} deformation modes.

Rocking modes

The bands observed for the rocking modes are in good agreement with those reported earlier (Table S5). The ν_{19} and ν_5 modes were observed at 835 cm^{-1} for the gas phase and at 838 cm^{-1} for the liquid spectrum. They, together with the ν_aGeC_3 mode, constitute the most intense bands of the infrared spectrum. In contrast, the Raman spectrum shows a very low intensity band at 828 cm^{-1}. Figure S3 shows the predicted position and relative intensities for the bands in this region. The shoulder that appears in the IR spectra of the gas at 876 cm^{-1} was not considered in the assignment because the splitting predicted by Yoshida for the ν_{19} and ν_5 modes is significantly lower (10 cm^{-1}) than that observed experimentally between the shoulder and the band at 835 cm^{-1} (41 cm^{-1}). In the spectrum of the liquid, the band and the shoulder appear at 838 and 854 cm^{-1}, respectively. The other scaling methods predict a splitting of 11 cm^{-1} for these modes (Table S4). However, a shoulder on the high wavenumber side at 830 cm^{-1} was found in the infrared spectra of the solid (Fig. S3). The splitting between that and the band at 844 cm^{-1} is closer to that predicted by the calculations and therefore was assigned to the ν_5 and ν_{19} CH_3 rocking modes, respectively.

The band that occurs at 762 cm^{-1} in the infrared spectrum was attributed to the remaining CH_3 rocking mode (ν_{20}), which became more intense in the gas phase infrared spectrum and shifted to 767 cm^{-1} in the solid state spectra. In the Raman spectra, this band displays a very low intensity, as well as the above-mentioned rocking modes, appearing at 761 cm^{-1}. The 6-31G* combination predicts a lower intensity for this band with respect to the experimental infrared spectra, as can be seen in Fig. S3.

CH_3 torsional modes

The torsional mode ν_{12} belongs to the A_2 symmetry species and is both infrared and Raman inactive; therefore, only the ν_{24} torsional mode belonging to E symmetry is expected to be observed in the vibrational spectra. A very low intensity band at 122 cm^{-1} was found in the Raman spectrum. A brief look at Table S1 shows that, except of the 6-31G, 6-31G*, 6-31+G and 6-31+G* basis sets, all the others predict the C–H torsional mode around 115–120 cm^{-1}. Taking this into consideration, we propose that

the band at 122 cm^{-1} can be assigned to the ν_{24} torsional mode. This is in accord with the bands observed for the chlorine (Roldán *et al*., under publication) and the iodine[31] compounds at 125 and 112 cm^{-1}, respectively. The higher shift of the CH_3 torsional mode to a low wavenumber for $(CH_3)_3GeI$ could be due to a slightly higher contribution of the iodine atom in this molecular vibration. Such an assumption is based on the analysis of the atomic displacement with the GaussView 3.0 program.[32]

GeC_3 group of modes and the Ge–Br stretching mode

Below 700 cm^{-1}, the stretching, deformation and rocking modes of the GeC_3 group are expected to appear. The bands located in this spectral region are in good agreement with those proposed earlier by other authors (Table S5). Only the ν_{21} antisymmetric and ν_6 symmetric GeC_3 stretching modes at 618 and 572 cm^{-1} for the liquid and the gas spectra could be observed in our RTIR spectrum because of the measured range. These bands slightly shift to 620 and 573 cm^{-1} for the condensed phase spectrum. In the Raman spectra, the ν_{21} mode was also observed at 618 cm^{-1}, whereas the ν_6 mode produces the strongest polarized and intense band of the whole spectrum at 573 cm^{-1}. The band observed at 262 cm^{-1} was directly assigned to the νGe–Br stretching mode, and the bands at 192 and 153 cm^{-1} were attributed to GeC_3 antisymmetric deformation (ν_{22}) and rocking (ν_{23}) modes, respectively, by comparison with the assignment from previous authors and the prediction from Yoshida's scaling (Fig. 5). The ν_8 GeC_3 symmetric deformation mode has not been observed so far. However, its value can be estimated from the theoretical calculations. Figure 5 compares the predicted bands in this region with the ones experimentally observed, and Table S4 displays the estimated wavenumbers for this mode from all the scaling procedures used in this work. Pulay's scaling predicts that this band almost overlaps with the GeC_3 rocking mode at 573 cm^{-1}, whereas Pongor's scaling predicts this band to be closer to the GeC_3 antisymmetric deformation at 192 cm^{-1}. Finally, the SQM force field obtained after the refinement of the scale factors gives a wavenumber value of 181 cm^{-1}. This value is in agreement with that observed at 188 cm^{-1} for $(CH_3)_3GeCl$ and at 176 cm^{-1} for $(CH_3)_3GeI$.

The assignments for the combination and overtone modes observed for the gas and liquid phase of BTMG are based on the assignments already proposed for the chloro (Roldán *et al*., under publication) and iodine[31] compounds and are listed in Table S6 (Supporting Information).

Force Constants Calculation

In this section, the valence force constants of BTMG were calculated by adjusting the theoretical force field by means of refined scale factors in order to improve the reproduction of the experimental wavenumbers. The scale factor values proposed by Kalincsák and Pongor[18] defined for the B3LYP/6-31G* level of theory were used as initial values for all the vibrational modes and are shown in Table 2. Since these scale factors are not defined for compounds containing Ge and Br atoms, we propose their refinement for this molecule using the multiple scaling SQM methodology[14–16] (Computational Details section). Thus, the scale factors were initially grouped according to the nature and symmetry of the vibrational modes of the molecule, and refined by using an iterative least-squares procedure. Then, the refined scale factors were used to scale the B3LYP/6-31G* force field for BTMG and obtain the scaled wavenumbers, which are shown in Table S4. For the inactive A_2 modes the corresponding calculated wavenumbers were used because no data were available. The resulting set of 11 refinement scale factors (Table 2) was used to scale the B3LYP/6-31G* force field, which decreased the RMSD from an initial value of 26.6 cm^{-1} to a final value of 8.1 cm^{-1}. As can be observed from Table S4, the use of the different scaling methods reduces the larger deviations observed especially in the C–H vibration regions. The B3LYP/6-31G* method predicts vibrational wavenumbers with an initial RMSD of 96.1 cm^{-1}, and decreases to 24.3 cm^{-1} by using the transferable Rauhut and Pulay[15] scale factors, to 26.6 cm^{-1} by using the Kalincsák and Pongor[18] scale factors, and finally to 8.1 cm^{-1} by using the refined scale factors. In addition, the vibrational wavenumbers predicted from the B3LYP/6-311+G** method were calculated with an initial RMSD of 71.9 cm^{-1}, decreasing to 18.5 cm^{-1} after the Yoshida *et al*. scaling.[17]

Table 2. Refined scale factors from the BTMG force field calculated with B3LYP/6-31G*

Vibrational mode[a]	Scale factor	
	Initial[b]	Final[c]
ν_a CH_3	0.920	0.897
ν_s CH_3	0.920	0.903
δ_a CH_3	0.915	0.870
δ_s CH_3	0.915	0.883
ρ CH_3	0.915	0.885
ν_a GeC_3	1.042	0.957
ν_s GeC_3	1.042	0.957
ν GeBr	1.069	0.895
δ_a GeC_3	1.218	1.150
δ_s GeC_3	1.218	1.150
ρ GeC_3	1.218	1.070
τ CH_3	0.831	0.800

[a] ν, stretching; δ, angular deformation; ρ, rocking; τ, torsion; s, symmetric; a, antisymmetric.
[b] Kalincsák and Pongor's scale factors, from Ref. [18].
[c] Obtained after the refinement in this work.

The harmonic force constants before (initial) and after (final) the refinement procedure calculated with the B3LYP/6–31G* method are shown in Table 3, along with those reported by Imai *et al*.[13] The refinement of Kalincsák and Pongor's[18] scale factors produces fundamentally an adjustment on the GeBr and GeC force constant values, which is accompanied by a decrease of the RMSD from 26.6 to 8.1 cm^{-1}. The PED among the vibrational modes obtained from the SQM scaling is given in Table S4. A small number of vibrational modes are predicted to be pure modes described by a single symmetry coordinate, such as the GeBr stretching (ν_7), and those that involve the motions of the GeC_3 group (ν_6, ν_8, ν_{21}, ν_{22}). The remaining modes are strongly mixed among modes of closer wavenumbers.

Conclusions

- Because the BTMG compound is used in diverse synthetic reactions in organic chemistry, the study of its bond force and characterization by means of infrared and Raman spectroscopy

Table 3. Selected internal force constants for BTMG calculated with B3LYP/6-31+G*, along with the previously reported values

Coordinate	Force constant[a]		
	Initial[b]	Final[c]	Imai[d]
f(CH)	4.945	4.82	–
f(GeC)	2.965	2.723	2.75
f(CH/CH)	0.039	0.036	–
f(GeC/GeC)	0.023	0.021	–
f(GeBr)	1.959	1.639	1.61
f(CGeC)	0.539	0.485	–
f(CGeBr)	0.643	0.569	–
f(HCH)	0.434	0.417	–
f(HCGe)	0.370	0.355	–
f(HCGeBr)	0.042	0.040	–
f(CGeC/CGeC)	−0.058	−0.068	–
f(CGeBr/CGeBr)	−0.110	−0.111	–
f(HCH/HCH)	−0.099	−0.094	–
f(HCGe/HCGe)	−0.067	−0.062	–

[a] Units are mdyn $Å^{-1}$ for stretchings, stretching/stretching interactions and mdyn Å rad^{-2} for deformations and deformation/deformation interactions.
[b] Calculated by using Kalincsák and Pongor's scale factors included in Table 2.
[c] Calculated using the scale factors obtained after the refinement procedure in this work.
[d] Calculated with Wilson's G–F matrix method, taken from Ref. [13].

are of great importance in order to understand the reactions in which it is involved.

- Therefore, the liquid, gas and solid infrared spectra along with the Raman spectra were recorded for BTMG. Low temperature techniques as well as the application of the FSD to the Raman spectrum allowed achieving the maximum amount of information. These new spectroscopic data along with the theoretical prediction of the vibrational spectra for BTMG using different scaling methods with B3LYP calculations led us to propose assignments for those vibrational modes of closer wavenumbers.
- The experimental wavenumbers were better estimated by a combination of the B3LYP method and the higher-size basis sets such as 6-311+G** and 6-311++G**. The cc-PVDZ and cc-PVTZ basis sets give similar results in predicting the vibrational wavenumbers. The use of different scaling procedures produced an improvement in the quality of the predicted wavenumbers, which is in accord with a decrease of the RMSD values. The deviation of the calculated wavenumbers diminish from 96.1 cm^{-1} for B3LYP/6-31G* and 71.9 cm^{-1} for B3LYP/6-31G*, to 24.3 cm^{-1} for the scaling procedure by using the Rauhut and Pulay[15] factors, 26.6 cm^{-1} for the scaling procedure by using the Kalincsák and Pongor[18] scale factors and 18.5 cm^{-1} with the WLS method, until reaching a final value of 8.1 cm^{-1} when the Kalincsák and Pongor[18] scale factors where refined.
- The prediction of the relative intensities was better for the infrared than for the Raman spectrum for both levels of theory (B3LYP/6-31G* and B3LYP/6-311+G**). The WLS method gave better results in simulating the C–H vibration region. Some better results were obtained with the SQM scaling for the GeC_3 vibrational modes.
- The force constants for BTMG were calculated by scaling the B3LYP/6-311+G** molecular force field with the resulting refined scale factors through the SQM methodology. This scaled force field reproduced the 19 observed vibrational wavenumbers by using a set f 11 scale factors with a final deviation of 8.1 cm^{-1}. A comparison with the predicted values shows excellent agreement for the calculated wavenumbers with the experimental ones.

Supporting information

Supporting information may be found in the online version of this article.

Acknowledgements

The authors thank CIUNT (Consejo de Investigaciones, Universidad Nacional de Tucumán) and CONICET (Consejo Nacional de Investigaciones Científicas y Técnicas, R. Argentina, PIP CONICET 6457) for financial support.

References

[1] L. M. Dennis, W. I. Patnode, *J. Am. Chem. Soc.* **1930**, *52*, 2778.
[2] V. F. Mironov, A. L. Kravchenko, *Izv. Akad. Nauk SSSR* **1965**, *6*, 1026.
[3] Y. Yamamoto, S. Hatsuya, J. Yamada, *J. Chem. Soc., Chem. Commun.* **1988**, 1639.
[4] E. Piers, P. C. Marais, *J. Org. Chem.* **1990**, *55*, 3454.
[5] D. M. Schubert, A. D. Norman, *Inorg. Chem.* **1985**, *24*, 1107.
[6] W. J. Meyerhoffer, M. M. Bursey, *J. Organomet. Chem.* **1989**, *373*, 143.
[7] Y. S. Li, J. R. Durig, *Inorg. Chem.* **1973**, *12*(2), 306.
[8] K. Aarset, E. M. Page, *J. Phys. Chem. A* **2004**, *108*, 5474.
[9] M. I. Batuev, V. A. Ponomarenko, A. D. Matvecva, G. Vzenhovo, *Isv. Akad. Nauk SSSR* **1959**, 2120.
[10] V. E. Mironov, A. L. Kravchenko, *Izv. Akad. Nauk SSSR* **1965**, 988.
[11] D. F. Van de Vondel, G. P. Van der Keler, G. Van Hooydonk, *J. Organomet. Chem.* **1970**, *23*, 431.
[12] J. R. Durig, S. M. Craven, J. Bragin, *J. Chem. Phys.* **1969**, *51*(12), 5663.
[13] Y. Imai, K. Aida, K. Sohma, F. Watari, *Polyhedron* **1982**, *1*(4), 397.
[14] P. Pulay, G. Fogarasi, G. Pongor, J. E. Boggs, A. Vargha, *J. Am. Chem. Soc.* **1983**, *105*, 7037.
[15] G. Rauhut, P. Pulay, *J. Phys. Chem.* **1995**, *99*, 3093.
[16] G. Rauhut, P. Pulay, *J. Phys. Chem.* **1995**, *99*, 14572.
[17] H. Yoshida, K. Takeda, J. Okamura, A. Ehara, H. Matsuura, *J. Phys. Chem.* **2002**, *106*, 3580.
[18] F. Kalincsák, G. Pongor, *Spectrochim. Acta, Part A* **2002**, *58*, 999.
[19] J. K. Kauppinen, D. J. Moffatt, H. H. Mantsh, D. G. Cameron, *Appl. Spectrosc.* **1981**, *35*, 271.
[20] J. K. Kauppinen, D. J. Moffatt, D. G. Cameron, H. H. Mantsh, *Appl. Opt.* **1981**, *20*, 1866.
[21] J. K. Kauppinen, D. J. Moffatt, M. R. Holberg, H. H. Mantsh, *Appl. Spectrosc.* **1991**, *45*, 411.
[22] *FTIR spectrophotometer software, Spectrum Version 5.3*, Perkin Elmer: © **2005**.
[23] M. J. Frisch, G. W. Trucks, H. B. Schlegel, G. E. Scuseria, M. A. Robb, J. R. Cheeseman, J. A. Montgomery Jr, T. Vreven, K. N. Kudin, J. C. Burant, J. M. Millam, S. S. Iyengar, J. Tomasi, V. Barone, B. Mennucci, M. Cossi, G. Scalmani, N. Rega, G. A. Petersson, H. Nakatsuji, M. Hada, M. Ehara, K. Toyota, R. Fukuda, J. Hasegawa, M. Ishida, T. Nakajima, Y. Honda, O. Kitao, H. Nakai, M. Klene, X. Li, J. E. Knox, H. P. Hratchian, J. B. Cross, C. Adamo, J. Jaramillo, R. Gomperts, R. E. Stratmann, O. Yazyev, A. J. Austin, R. Cammi, C. Pomelli, J. W. Ochterski, P. Y. Ayala, K. Morokuma, G. A. Voth, P. Salvador, J. J. Dannenberg, V. G. Zakrzewski, S. Dapprich, A. D. Daniels, M. C. Strain, O. Farkas, D. K. Malick, A. D. Rabuck, K. Raghavachari, J. B. Foresman, J. V. Ortiz, Q. Cui, A. G. Baboul, S. Clifford, J. Cioslowski, B. B. Stefanov, G. Liu, A. Liashenko, P. Piskorz, I. Komaromi, R. L. Martin, D. J. Fox, T. Keith, M. A. Al-Laham, C. Y. Peng, A. Nanayakkara, M. Challacombe, P. M. W. Gill, B. Johnson, W. Chen, M. W. Wong, C. Gonzalez, J. A. Pople, *Gaussian 03, Revision B.01*, Gaussian: Pittsburgh, **2003**.

[24] J. Hehre, L. Random, P. V. R. Scheleyer, J. A. Pople, *Ab-initio Molecular Orbital Theory*, Wiley-Interscience: New York, **1986**.
[25] T. H. Dunning Jr, *J. Chem. Phys.* **1989**, *90*, 1007.
[26] D. E. Woon, T. H. Dunning Jr, *J. Chem. Phys.* **1993**, *98*, 1358.
[27] R. A. Kendall, T. H. Dunning Jr, R. J. Harrison, *J. Chem. Phys.* **1992**, *96*, 6796.
[28] P. Pulay, G. Fogarasi, F. Pang, J. E. Boggs, *J. Am. Chem. Soc.* **1979**, *101*(10), 2550.
[29] W. B. Collier, *Program FCARTP (QCPE #631)*, Department of Chemistry, Oral Roberts University: Tulsa, **1992**.
[30] C. E. Blom, C. Altona, *Mol. Phys.* **1976**, *31*, 1377.
[31] M. L. Roldán, S. A. Brandán, S. L. Masters, D. A. Wann, H. E. Robertson, D. W. H. Rankin, A. Ben Altabef, *J. Phys. Chem. A* **2007**, *111*, 7200.
[32] B. Nielsen, A. J. Holder, *GaussView 3.0, User's Reference*, Gaussian: Pittsburgh, **2003**.